Journal of Alloys and Compounds 504S (2010) S395–S398

Contents lists available at ScienceDirect

Journal of Alloys and Compounds

journal homepage: www.elsevier.com/locate/jallcom

Cross-sectional transmission electron microscopy studies for deformation behaviors of AlN thin films under Berkovich nanoindentation

Sheng-Rui Jian[a,*], G.-J. Chen[a], H.-G. Chen[a], Jason S.-C. Jang[b], Y.-Y. Liao[c], P.-F. Yang[d], Y.-S. Lai[d], M.-R. Chen[e], H.-L. Kao[e], J.-Y. Juang[f]

[a] Department of Materials Science and Engineering, I-Shou University, Kaohsiung 840, Taiwan
[b] Department of Mechanical Engineering; Institute of Materials Science & Engineering, National Central University, Chung-Li 320, Taiwan
[c] Department of Applied Physics, National University of Kaohsiung, Kaohsiung 81148, Taiwan
[d] Central Product Solutions, Advanced Semiconductor Engineering, Inc., 26 Chin 3rd Road, Nantze Export Processing Zone, Kaohsiung 811, Taiwan
[e] Department of Electronic Engineering, Chung Yuan Christian University, Chung-Li 32023, Taiwan
[f] Department of Electrophysics, National Chiao Tung University, Hsinchu 300, Taiwan

ARTICLE INFO

Article history:
Received 1 July 2009
Received in revised form 27 January 2010
Accepted 10 February 2010
Available online 18 February 2010

Keywords:
AlN
Nanoindentation
Focused ion beam
Cross-sectional transmission electron microscopy

ABSTRACT

This article reports a nanomechanical response study of the contact-induced deformation behavior in AlN thin film by using a combination of nanoindentation and the cross-sectional transmission electron microscopy (XTEM) techniques. AlN thin films are deposited on Si(1 1 1) substrates by using the helicon sputtering system. The hardness and Young's modulus of the AlN thin film are measured by a Berkovich nanoindenter operated with the continuous contact stiffness measurements (CSM) mode. The obtained values of hardness and Young's modulus are 24.79 ± 0.33 GPa and 223.92 ± 5.34 GPa, respectively. XTEM samples are prepared by using focused ion beam (FIB) milling to accurately position the cross-section of the indented area. Although the film's surface was free from fracture, AlN thin film showed evidence of radial crack along the columnar grain boundary underneath the center of Berkovich indentation for an applied load of 100 mN. XTEM results also indicated that the slip bands on {1 1 1} planes and an indentation-induced phase transformation zone of silicon substrate, containing the metastable phases of Si-III and Si-XII, and, the amorphous phases are observed.

© 2010 Elsevier B.V. All rights reserved.

1. Introduction

With the tremendous progress of III-nitrides researches in both fundamental understanding and device application, AlN attracts much attention because of the direct wide band gap of about 6.2 eV at room temperature and some excellent characteristics for applications to solid-state light sources, such as laser diodes and light-emitting diodes, operating in the deep-ultraviolet spectral range [1,2]. Nevertheless, the successful fabrication of devices based on the AlN thin films requires better understanding of the mechanical properties in addition to its optical and electrical performances, since the contact loading during processing or packaging can significantly degrade the performance of these devices.

Nanoindentation has gained interest because it can clarify the mechanical properties (hardness and elastic modulus) of thin films while avoiding the effects from substrates [3,4]. The variation of these properties with the penetration depth, based on the respective analysis of load–displacement curves [5–8] while are also producing the contact-induced damage. However, the nanoindentation technique itself does not provide any information of nanoindentation-induced deformation mechanisms and dislocation propagation on the subsurface. The focused ion beam (FIB) miller, which is now used for a wide range of materials' characteristic applications [9], can be readily applied to image and prepare the cross-sections of materials. FIB can also be applied to prepare the lamella specimen of transmission electron microscopy (TEM), especially from samples which have been locally deformed. Consequently, the subsurface deformation mechanisms operating in both thin films and the substrates following nanoindentation can be observed using the FIB-based techniques.

Herein, we report, for the first time to our knowledge, cross-sectional transmission electron microscopy (XTEM) studies involving the deformation behavior of AlN thin films on Si(1 1 1) substrates following indentation with a Berkovich indenter and XTEM analyses. In this study, the use of the Berkovich indenter not only will reflect the more realistic situations that might be encountered in real applications but also will result in much higher local pressure with similar load, and hence, will be helpful in clarifying the pressure-induced phase transformation issue.

* Corresponding author. Tel.: +886 7 6577711x3130; fax: +886 7 6578444.
E-mail address: srjian@gmail.com (S.-R. Jian).

0925-8388/$ – see front matter © 2010 Elsevier B.V. All rights reserved.
doi:10.1016/j.jallcom.2010.02.050

2. Experimental details

Experimentally, AlN thin films are deposited on Si(1 1 1) substrates by using a helicon sputtering system. The helicon sputtering method involves a magnetron sputtering system enhanced with an inductively coupled RF plasma, in which sputtered atom can be ionized efficiently with coil power, and the plasma can be sustained at a gas pressure lower than that in conventional magnetron sputtering. Because the mean free path of the atoms can be increased to be larger than the target-to-substrate distance, a smooth surface and a good crystalline structure can thus be obtained at a low growth temperature. A 2-in. diameter Al target with a purity of 99.999% is employed as the cathode. After the sputtering chamber is evacuated to below 10^{-7} Torr, the sputtering gas consisting of a mixture of N_2 and Ar is introduced at various total sputtering pressures. The thin films are grown using the following sputtering parameters: the sputtering pressure of 1 mTorr, RF power of 150 W, sputtering gas mixture of Ar:N_2 = 1:3 and coil power of 50 W, and the substrate temperature is kept at 500 °C.

Depth-sensing indentation was used as the principal mechanical testing technique, using a Berkovich indenter tip of 50 nm radius (faces 65.3° from vertical axis). The experiments were conducted using an MTS Nano Indenter® XP instrument to obtain the mechanical characterizations of AlN thin film with the continuous contact stiffness measurements (CSM) procedures, which was accomplished by superimposing a small oscillation on the force signal and measuring the displacement response at the same frequency of 75 Hz. Firstly, the indenter was loaded and unloaded three times to ensure that the tip was properly in contact with the surface of the materials and that any parasitic phenomenon is released from the measurements. Then, the indenter was loaded for the fourth and final time at a strain rate of 0.05 s^{-1}, with a 60 s hold period inserted at peak load. The analytic method developed by Oliver and Pharr [10] was adopted to determine the hardness and Young's modulus of AlN thin film from the load–displacement curve. Also, in order to delineate the details of the contact-induced deformation mechanisms, direct microstructure observations, enabled by combining the focused ion beam and transmission electron microscopy techniques, were carried out.

In our measurements, firstly, a 10 × 5 indentation array with each indentation being separated by 50 μm to avoid inter-indent interactions was produced with an indentation load of 100 mN. In each indentation, the Berkovich diamond indenter was operated with the same loading/unloading rate (10 mN/s) and was held at the peak load for 30 s. The cross-sectional TEM samples were prepared from the indents by using a dual-beam FIB (Nova 220) station with Ga ions at 30 keV. Prior to milling, the FIB was used to deposit an ~1 μm thick layer of Pt to protect AlN thin film's surface. In addition, the details of FIB produced in preparing XTEM sample can be found elsewhere [9]. The XTEM lamella was examined in a FEI TECNAI G^2 TEM operating at 200 kV.

3. Results and discussion

The typical nanoindentation curve obtained for AlN thin film is shown in Fig. 1(a). The hardness and Young's modulus of AlN thin film can be calculated from the load–displacement records by means of the analytic method developed by Oliver and Pharr [10]. Moreover, with the continuous contact stiffness measurements, the CSM technique system is applied to record stiffness data along with load and displacement data dynamically, allowing hardness and Young's modulus to be calculated at every data point and averaged to acquire continuously during the indentation experiment. Therefore, the penetration depth dependence of the hardness and Young's modulus can be obtained, as shown in Fig. 1(b) and (c). While applying peak load of 4 mN, the relative mechanical properties are exhibited stably to converge during the loading–displacement process. When the mechanical properties obtained under nanoindentation process are measured from depths of 30–100 nm, then the obtained values of hardness and Young's modulus are 24.79 ± 0.33 GPa and 223.92 ± 5.34 GPa, respectively.

Taking into account that the load–displacement curve shown in Fig. 1(a), it is evident that there exists multiple discontinuities along the loading course (indicated by the arrows, referred to as multiple "pop-ins") and is reflecting the process of plastic deformation in the investigated material. This observation is in contrast to that reported in the previous study of AlN thin films [11], where no "pop-in" event was observed. The origin of this discrepancy is not clear at present. We speculate that different operating modes may lead to the dissimilar nanoindentation results.

The typical nanoindentation results obtained with a maximum load of 100 mN and a deeper penetration depth of ~900 nm is shown in Fig. 2. Although the resolution was much reduced because of the larger indentation load, similar multiple "pop-ins" are evident. The fact that multiple "pop-ins" are observable over such a wide range of indentation load and penetration indicates the close relations of AlN thin film to the plastic deformation. Since the multiple pop-ins are randomly distributed on the loading curve in Figs. 1(a) and 2, and each curve is associated with a different stress rate which increases with the maximum indentation load, it is suggestive that the first pop-in is not thermally activated. Instead, these phenomena are usually attributed to dislocation nucleation/propagation and slip during loading as have been observed in a wide variety of materials [8,9,12]. Thus, it is clear that the first pop-in event may reflect the transition from perfectly elastic to plastic deformation, that is, it is the onset of plasticity in AlN thin film. The corresponding shear stress under the Berkovich indenter at indentation load P^*, where the load–displacement discontinuity occurs, can be determined by using the following relation [13]:

$$\tau_{max} = 0.31\left(\frac{6P^*E^2}{\pi^3R^2}\right)^{0.33} \qquad (1)$$

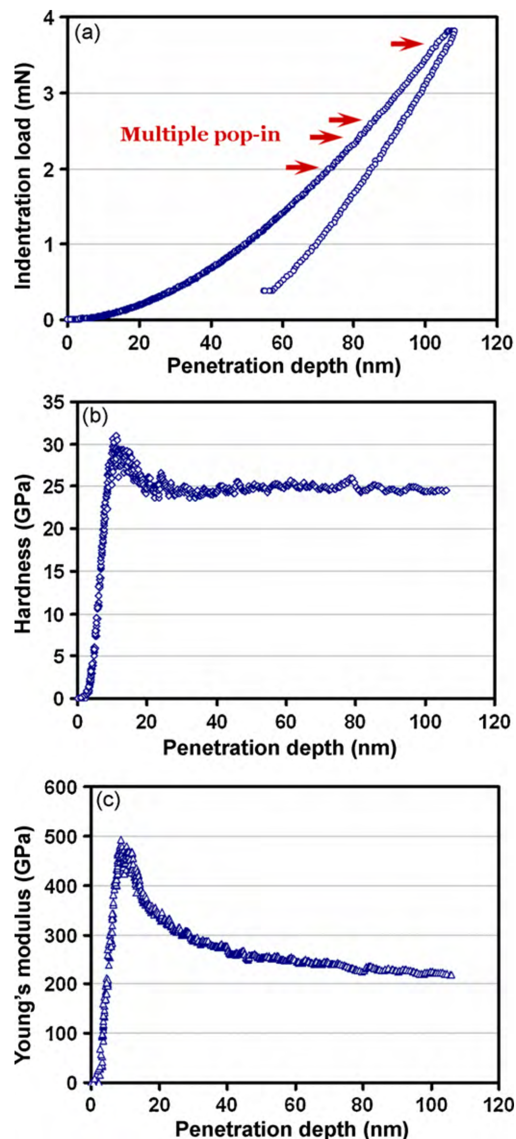

Fig. 1. Nanoindentation measurement results: (a) a typical load–displacement curve of AlN thin film showing the multiple "pop-ins" phenomena during loading (please see the arrows); (b) hardness–displacement curve, and (c) Young's modulus–displacement curve for AlN thin film.

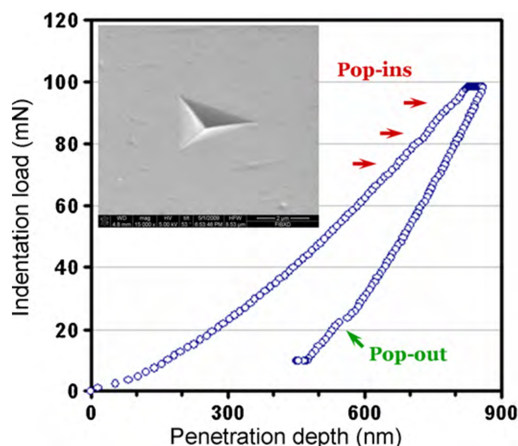

Fig. 2. SEM micrograph of a Berkovich indentation (please see the inset figure) on AlN thin film obtained at an indentation load of 100 mN, and the multiple "pop-ins" and "pop-out" phenomena displayed in the load–displacement curve.

where R is the radius of the tip of the indenter, and E is defined in terms of Young's moduli and Poisson's ratios of the diamond indenter and thin film. The maximum shear stress, τ_{max}, of AlN thin film is 25.42 GPa.

On the other hand, it is interesting to note that the load–displacement curve in Fig. 2 exhibits a significant discontinuity (namely, "pop-out") event on unloading. In 2005, Yan et al. [14] reported that pop-out event suddenly occurred with the low loading/unloading rate around a loading of 15–20 mN during unloading process. Moreover, it has been attributed to the formation of metastable phases of Si-III and Si-XII from Si-II as well. In addition, Domnich and Gogotsi [15] indicated that with slower loading/unloading rates led to the pop-out event during unloading step. This result should be induced by a sudden volume increase and the uplift of the material around the indenter as gradually decreased loading and, therefore the evidence of phase transformation is displayed at low load level during unloading. From the insert of Fig. 2, scanning electron microscopy (SEM) observations do not provide for such load (100 mN) any evidence of dislocation activity and crack features at the film's surface around the indentation, and even related to phase transformations beneath the Berkovich indenter. Therefore, the indentation-induced plastic deformation process is complex and further studies will be necessary to delineate what happens to the material as the indenter penetrates into the surface and/or substrate. The Berkovich nanoindentation-induced deformation mechanisms will be discussed in more detail with the aid of XTEM techniques in the following sections.

A bright-field XTEM image of AlN thin film after being indented with an indentation load of 100 mN is displayed in Fig. 3. No delamination was observed in the film/substrate interface, suggesting good interfacial bonding. And, the selected area diffraction (SAD) is displayed to indicate the Berkovich indentation-induced deformed zone: (I) and (II). We do not observe any halo rings in SAD (I) of Fig. 3, therefore, we can say that AlN thin film did not undergo the amorphization. In this case of SAD (I), it is taken with an aperture of similar diameter to the column showing the streaking of the diffraction spots corresponding to the rotation of the crystallographic planes. The SAD (II) from the deformed zone displayed strong rings corresponding to the amorphous silicon as well as additional reflections consistent with the presence of high-pressure phases, namely Si-III (BC8) and Si-XII (R8), similar to the previous studies for Berkovich nanoindentation on uncoated silicon [8,16]. The presence of a large amount of amorphous silicon, rather than the mixture phases of BC8 and R8, is attributed to the indentation load being insufficient for complete transformation. Therefore, this is consistent with the corresponding unloading curve showing a "pop-out" characteristic, as displayed in Fig. 2.

Surrounding the pyramidal shape transformed zone in silicon substrate, the dislocations activity phenomena can be observed significantly in Fig. 3. Slip bands, as well as dislocations on {1 1 1} planes of silicon substrate, are also seen. The material around the indent is highly stressed as a result of the phase transformation, leading to the bend contours phenomena. This stress was not relieved by cutting the edges of foil in the course of FIB process. In addition, it is interesting to note that a median crack is formed at the bottom of the transformation zone, which extends approximately 1.5 μm. The formation of the median crack beneath the slip band apex indicates increased stress concentrations in this locally region. The accumulated dislocations can concentrate shear stresses at the slip band extremity and, further cause the nucleation of a crack [17].

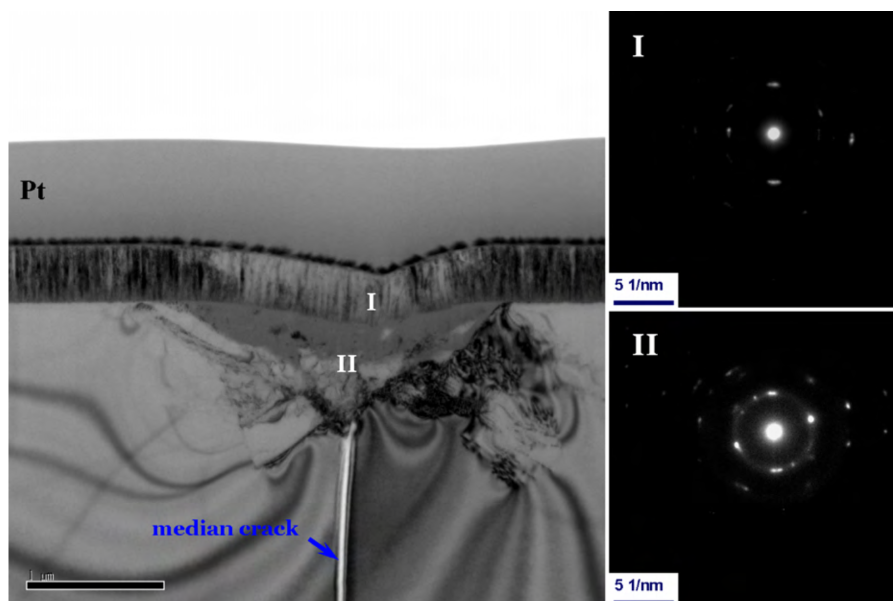

Fig. 3. XTEM image of sample after an indentation load of 100 mN. And, selected area diffraction pattern results of sample underneath the Berkovich indent from the (I): indented AlN thin film and (II): transformation zone in Si substrate.

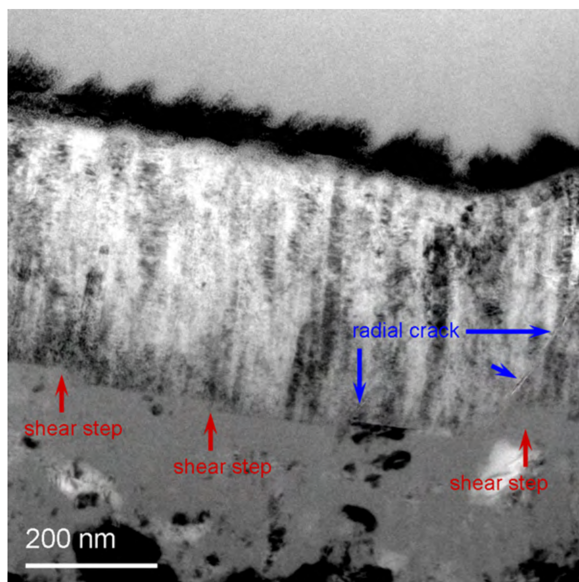

Fig. 4. A close-up view of XTEM image of the deformed zone of AlN thin film, showing that the cracking along the intercolumnars were located within the films layer.

In order to have a closer look at the Berkovich indentation-induced deformation immediately beneath the tip, Fig. 4 shows an enlarged XTEM image in the vicinity of the tip contact region. It can be seen that the radial cracks appeared to initiate at the films/substrate interface, most likely owing to the local stress concentrations. Of particular interest is the fact that the intercolumnar shear steps can be observed at the interface near the center of the impression. In this extensive deformation region, the stress distribution is expected to be compressive; while, the interface is presumably dominated by a tensile stress [13]. During the course of indentation, the tangential traction that occurs at the surface of adjacent columns to their relatively vertical displacement and the generation of shear steps. Therefore, the behaviors of shear steps in the high compressive region are considered to be in the sliding mode, corresponding to longitudinal shearing of the columnar boundaries in a direction normal to the crack front [18].

In closing, from the above observations and discussion, it is apparent that, in the Berkovich nanoindentation scheme, the multiple "pop-ins" are usually observed after permanent plastic deformation has occurred and two of the possible mechanisms, the shear sliding of adjacent intercolumnars and radial crack from films/substrate interface, were basically ruled out. In addition, this is may be due, in part, to some of the sudden expansion caused by the transformation Si-I → Si-II is partially accommodated by films, which results in the multiple "pop-ins". On indentation to 100 mN, increased the high compressive plastic strain in AlN thin film to ∼40%, resulting in significant bending at the interface together with radial cracks and shear steps (as shown in Fig. 4); the effects of indentation have, in fact, extended into the silicon substrate. A Berkovich nanoindentation-induced transformed zone, containing the metastable phases of Si-III and Si-XII, and the amorphous phases are observed. Therefore, the presence of "pop-out" event in the load–displacement curve can be attributed to the deformation mechanisms, that is, indentation-induced phase transformation, operating in the silicon substrate.

4. Conclusions

In summary, the mechanical responses of AlN thin films deposited on Si(1 1 1) substrate to Berkovich nanoindentation and microscopic techniques. XTEM revealed dislocations, a median crack and slip bands on {1 1 1} planes of the silicon substrate. At an indentation load of 100 mN, a Berkovich nanoindentation-induced transformation zone, containing the metastable phases of Si-III and Si-XII, and the amorphous phases are observed. In addition, the plastic deformation mechanisms consisted of radial crack propagation from the films/substrate interface and shear sliding along the adjacent intercolumnar are observed in indented AlN thin film. The hardness and Young's modulus of AlN thin film estimated using the continuous stiffness operation mode provided with the Berkovich nanoindenter are 24.79 ± 0.33 GPa and 223.92 ± 5.34 GPa, respectively.

Acknowledgements

This work was partially supported by the National Science Council of Taiwan and I-Shou University, under Grant Nos.: NSC 97-2218-E-214-003, NSC 97-2112-M-214-002-MY2, ISU97-07-01-01, ISU97-07-01-04 and ISU 97-S-02.

References

[1] Y. Taniyasu, M. Kasu, T. Makimoto, Nature 441 (2006) 325.
[2] J. Li, Z.Y. Fan, R. Dahal, M.L. Nakarmi, J.Y. Lin, H.X. Jiang, Appl. Phys. Lett. 89 (2006) 213510.
[3] X.D. Li, B. Bhushan, Thin Solid Films 377–378 (2000) 401.
[4] S.R. Jian, J.S.C. Jang, G.J. Chen, H.G. Chen, Y.T. Chen, J. Alloys Compd. 479 (2009) 348.
[5] X.D. Li, L. Zhang, H.S. Gao, J. Phys. D: Appl. Phys. 37 (2004) 753.
[6] B. Haberl, J.E. Bradby, S. Ruffell, J.S. Williams, P. Munroe, J. Appl. Phys. 100 (2006) 013520.
[7] S.R. Jian, Appl. Surf. Sci. 254 (2008) 6749.
[8] S.R. Jian, J.S.C. Jang, J. Alloys Compd. 482 (2009) 498.
[9] C.H. Chien, S.R. Jian, C.T. Wang, J.Y. Juang, J.C. Huang, Y.S. Lai, J. Phys. D: Appl. Phys. 40 (2007) 3985.
[10] W.C. Oliver, G.M. Pharr, J. Mater. Res. 7 (1992) 1564.
[11] X.H. Ji, S.P. Lau, G.Q. Yu, W.H. Zhong, B.K. Tay, J. Phys. D: Appl. Phys. 37 (2004) 1472.
[12] D.F. Bahr, D.E. Kramer, W.W. Gerberich, Acta Mater. 46 (1998) 3605.
[13] K.L. Johnson, Contact Mechanics, Cambridge University Press, Cambridge, UK, 1985.
[14] X.Q. Yan, X.M. Huang, S. Uda, M.W. Chen, Appl. Phys. Lett. 87 (2005) 191911.
[15] V. Domnich, Y. Gogotsi, Appl. Phys. Lett. 76 (2000) 2214.
[16] I. Zarudi, L.C. Zhang, W.C.D. Cheong, T.X. Yu, Acta Mater. 53 (2005) 4795.
[17] A.N. Stroh, Proc. R. Soc. London, Ser. A 223 (1954) 404.
[18] S. Bhowmick, A.N. Kale, V. Jayaram, S.K. Biswas, Thin Solid Films 436 (2003) 250.